Available online at www.jourcc.com

Journal homepage: www.JOURCC.com

Journal of Composites and Compounds

Synthesis of Zn-Co-TiO_2 nanocomposite coatings by electrodeposition with photocatalytic and antifungal activities

Mehdi Reisi Nafchi [a], Reza Ebrahimi-kahrizsangi [a]*

[a] *Advanced Materials Research Center, Department of Materials Engineering, Najafabad Branch, Islamic Azad University, Najafabad, Iran*

ABSTRACT

TiO_2 has become the most well-known photocatalysts for solving environmental problems as a wide-band n-type semiconductor. This research aimed to coat a carbon steel substrate with Zn-Co-TiO_2 nanocomposite via the electrodeposition method. Scanning electron microscopy (SEM) was used to examine the microstructure, (energy-dispersive X-ray spectroscopy) EDS analysis was used to examine the composition of the coating, and a pull-off test was used to determine the adhesion of the coating. In this regard, the electrodeposition of the coatings was carried out at the optimum conditions of 0.1 A, the concentration of TiO_2 equal to 15 g/L, deposition time of 20 min, the temperature of 25.5 °C, and pH of 5-5.5 in different electrolyte compositions. Also, the photocatalytic properties of TiO_2 were determined by the fungal growth on the sample surface. According to the results, the fungal growth was reduced with the increase in the TiO_2 content in the coating.

Peer review under responsibility of JCC Research Group

ARTICLE INFORMATION

Article history:
Received 1 August 2021
Received in revised form 27 September 2021
Accepted 14 November 2021

Keywords:
Adhesion
Electrical deposition
Anti-fungal properties
Nanocomposite
Zn-Co-TiO_2

1. Introduction

In recent decades, TiO_2, as a wide bandgap n-type semiconductor, has become one of the most well-known photocatalysts for solving environmental problems [1, 2]. Furthermore, TiO_2 photocatalytic goods such as antifungal, antiviral, surface sterilization tools, and self-cleaning glass have been shown to be effective and of considerable value for the applications in which they are directed to photocatalytic activity based on the bandgap energy of materials [3]. TiO_2 has two phases: rutile and anatase which show a bandgap in 3 and 3.2 eV [1, 4, 5]. As a result, TiO_2 is known to have photocatalytic characteristics in ultraviolet (UV) light irradiation, whereas doping compounds alter the TiO_2 structure to give photocatalytic activity in visible light. Bulk TiO_2 has low photocatalytic potential, regardless of the kind of TiO_2 (anatase and rutile TiO_2 are the most commonly reported photocatalysts) [6]. Due to their high surface-to-volume ratio, improved charge transport, increased number of delocalized carriers on the surface, improved lifetime obtained by their dimensional anisotropy, and the effective distribution for the separation of electrons and holes as shown by photo magnification, TiO_2 nanocrystals have several advantages over their bulk counterparts in terms of potential applications [1, 7].

Because of their corrosion resistance, electrodeposited Zn and Zn alloy coatings can be utilized as aesthetic coatings, although they are most commonly employed as protective coatings [8, 9]. The corrosion resistance of Zn alloy coatings on steel can be up to 10 times higher than that of pure zinc coatings. Zn-Co, Zn-Ni, Zn-Sn, Zn-Fe, and Zn-Mn, are the most studied zinc alloys formed via electrodeposition [10-12]. According to Brenne's classification, Zn-Co alloy electrodeposition proceeds by anomalous co-deposition, suggesting preferential deposition of the less noble metal (Zn) over the nobler metal (Co) under a wide range of plating conditions [11].

Chemical and electrochemical procedures are two of the most fundamental approaches for creating composite coatings. The chemical composition of composite coatings provides low porosity for unparalleled application. The solutions utilized in such procedures, on the other hand, are costly and unstable. Furthermore, the chemical application of coatings occurs at high temperatures. Applying composite coatings by the electrochemical method is significantly faster than other chemical methods. Furthermore, the electrodeposition of coatings is defined by the technical process's manageability and reliability [13-15].

The use of electrodeposition has been established as a cost-effective technique for fabricating nanocomposite coatings with homogeneous dispersion of semiconductor particles (i.e., TiO_2) in a metal matrix, such as nanocomposite coatings with homogeneous semiconductor particles dispersion (i.e., TiO_2) in a metal matrix. It has been shown that the photocatalytic activity of TiO_2-based composite coatings is influenced by the matrix's composition, particularly for metal matrix composites that stimulate photocatalysis [1, 3, 14, 16]. Process parameters such as induced hydrodynamic conditions, deposition current density, type of applied current (direct or pulse), electrolyte pH value, additive presence, electrolyte compositions, and the characteristics of the reinforcing particles (surface charge, conductivity, size, etc.) and their concentration in the bath, all influence the electrodeposited composite coatings properties [1, 15, 17].

To the best of our knowledge, no previous paper has focused on the electrical deposition and simultaneous use of chemically modified TiO_2

* *Corresponding author: Mehdi Reisi Nafchi ; E-mail: mehdireisi62@gmail.com*
https://doi.org/10.52547/jcc.3.4.2

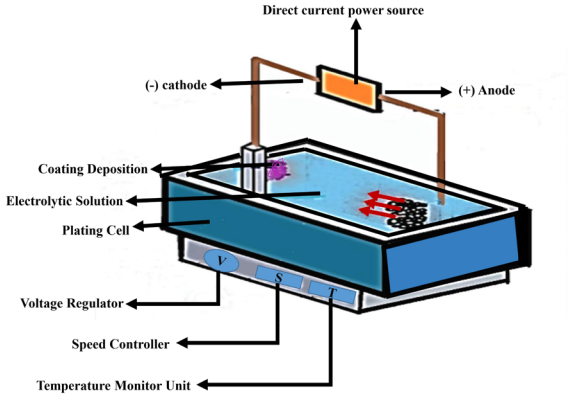

Fig. 1. Schematic of electrochemical deposition of nanocomposite on the metal surface.

particles in the Zn-Co matrix. Also, research on the photocatalytic activity and adhesion quality of this type of electrical coating has not been carried out by scientists [18, 19]. Therefore, in this research, Zn-Co-TiO_2 composite was coated on a mild steel substrate using an electrodeposition process under direct current (DC) conditions in a chloride solution.

The goal of this research is to create a functional composite composed of the Zn–Co matrix and TiO_2 particles. Chemically modified TiO_2 particles are added to provide photoactivity under UV irradiation for antifungal applications in wastewater and water. As a result, this research has two goals: (a) to determine the best electrodeposition parameters by adjusting particle concentration in the bath, resulting in Zn-Co-TiO_2 nanocomposite coatings with a high co-deposition percentage of TiO_2 particles dispersed in a metal alloy matrix. (b) Using the line scanning method of the cross-section, evaluate the morphological and microstructure properties of the coating, as well as the influence of the electrolyte bath concentration on adhesion coating.

2. Methods and materials

2.1. Substrate preparation

As substrates, mild steel plates with a diameter of 20 mm and a thickness of 2 mm were employed, while platinum plates with dimensions of 80 × 30 × 1 mm were used as anodes [20, 21]. Table 1 shows the nominal composition of mild steel plates. The anode was pure platinum and the cathode was mild steel plates (99.99 %). The mild steel specimens were manually polished using 80, 240, 800, 1200, and 2400 grit emery type abrasive papers, then degreased in 5 % NaOH at 60 °C for 30 minutes before being washed with water [22-24]. Sandblasting with aluminum oxide abrasive particles with a particle size of 70-80. Degreasing was performed with 5% sodium hydroxide solution [25].

2.2. Electrodeposition of the coatings

A mild steel substrate was activated by immersing in HCl solution (2 %) for 5 seconds at ambient temperature, then it was washed in distilled water. Before coating, the plating solution was prepared at room temperature using analytical grade chemicals and distilled water. The bath formulation was created a day before the coating procedure and

Table 1.
Nominal chemical composition (wt. %) of mild steel substrate.

Element	C	P	S	Ni	Mn	Si	Fe	Al
Composition %	0.15	0.01	0.031	0.008	0.45	0.18	Bal.	0.005

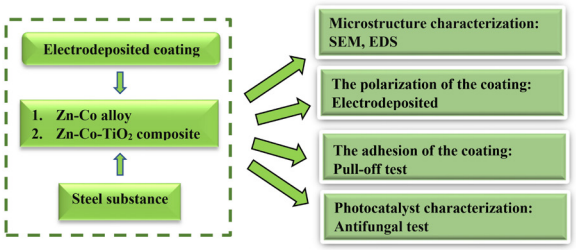

Fig. 2. Flowchart summarizing the characterization of the electrodeposited coatings.

stirred continuously at 200 rpm for suspension stability (to avoid particle agglomeration) and to improve the solution's electrophoretic mobility. Table 2 shows the chemical compositions of the bath. The addition of KCl was used primarily to boost the conductivity of the electrolyte. Before each electrodeposition experiment, the pH of the bath was adjusted to constant values in the range of 5-5.5.

Zn-Co and Zn-Co-TiO_2 alloy nanocomposite coating was deposited electrically on the mild steel with a geometry of (80 × 30 × 1) mm^3 from a sulfate bath. Zinc and cobalt are used as anode and cathode, respectively. The steel soft plates were mechanically polished by varying degrees of sandpaper to obtain a uniform and smooth surface. The samples were degreased in trichloroethylene vapors and HCl (10%) to clean any rust and dust. The plates were eluted by water, then air-dried, and dipped in the solution of a plating bath. The bath solution was kept at pH=5.5 using 10% $NaHCO_3$ and H_2SO_4. Before plating, the bath solution was stirred with a magnetic stirrer at 600 rpm for about 24 hours. The temperature was maintained at 25.5 °C during stirring and vibration. The density of current for plating was kept constant at 4 A/dm^2. Sedimentation was performed using a DC power supply under stagnant bath solution conditions. The electron deposition technique describes used to develop nanocomposites shown in Fig. 1 [10, 26, 27].

2.3. Characterization of electrodeposited coatings

After sample preparation, surface preparation and coating were performed by the electric deposition method. Electrolysis coating tests with polarity, microstructure morphology, adhesion test, and photocatalytic test were performed. Fig. 2. Explains the characterization of electrodeposited coatings in detail.

2.3.1. Microstructure study of the coatings

In the laboratory, cross-sections of the samples were prepared by a cutter with a speed of 3000 rpm. To determine the morphology and percentage of the TiO_2 particles, an EDS-equipped scanning electron microscope (SEM) (Coaxem CX100, South Korea) was used. A linear analysis of chemical elements that graphically determine the intensity of the elements in the coating was performed from the surface of the steel sample to the surface of the coating [28].

2.3.2. Adhesion test

To perform the adhesion strength test on the applied coatings, the tensile test according to the ASTM D4541 standard was used. For this purpose, parts called dolly with a diameter of 2.5 cm adhered to the nanocomposite coating with a strong adhesive of single-component epoxy with a strength of about 60 MPa (MPa) and then stretched under tensile force at a speed of 1 mm/min. The force required for separation is reported in MPa (MPa) [29, 30].

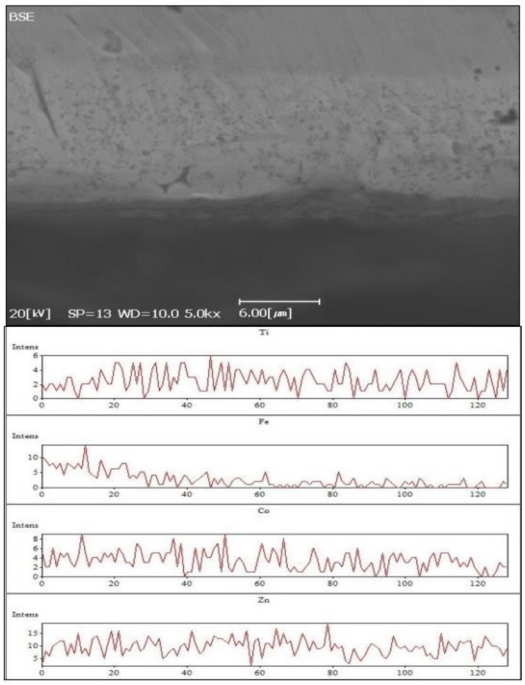

Fig. 3. Line scan analysis of the coating deposited in electrolyte B.

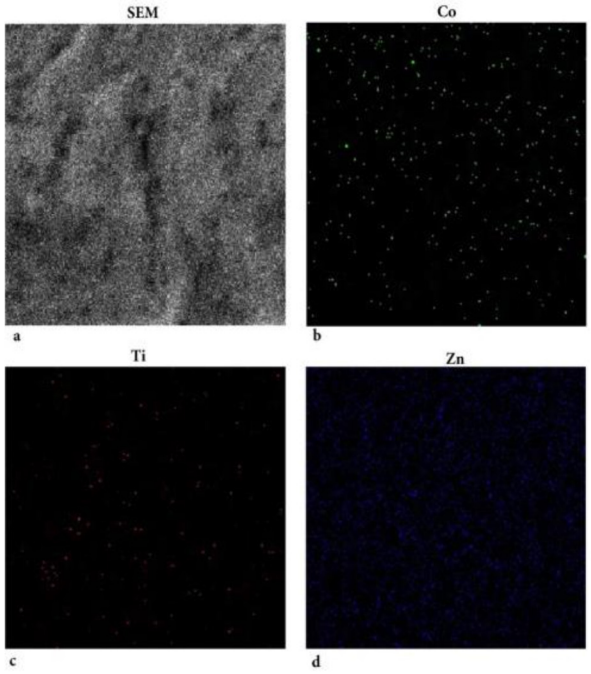

Fig. 4. SEM (a) and plane scan analysis of the cross-section of the coating deposited in electrolyte B (b-d).

2.3.3. Antifungal test

To evaluate the photocatalytic and anti-fungal properties, a test according to Fungus MIL-STD 810G Method 508.6 was used. In this test, the fungi growth on the sample surface was examined. The coated sample was placed in an environment containing 1,000,000 fungal eggs and moisture content less than 100% and more than 90% at 30 ° C for 21 days [31, 32].

3. Results and discussion

This section describes the characterization results of Zn, Co, and TiO_2 particles by EDS and SEM. In addition, the effect of Zn, Co, and TiO_2 nanoparticles on the electrical deposition of cobalt was analyzed by cathode curves polarization, cyclic studies of voltammogram. In addition, a nanocomposite of Zn, Co, and TiO_2 coatings was exposed to corrosion and examined under an adhesion test and photocatalytic test.

3.1. EDS analysis of the coatings

The elemental composition of the coatings obtained from EDS analysis is given in Table 3. As seen, the content of TiO_2 is dependent on the composition of the electrolyte. According to the table, the content of TiO_2 in the coatings deposited in electrolyte A is very low, and thereby, it is not a suitable composition according to the aim of this study. In order to deposit metals whose standard potentials are not the same or close to each other simultaneously by an electric deposition method, and change the potential difference between the two metals, the concentration of the electrolyte was changed. This change was used to increase the concentration of metal salts that have a lower standard potential than metal salts with higher standard potential in the electrolyte. In this regard, electrolyte B was prepared with a higher concentration of cobalt chloride salt than zinc chloride salt. Increasing the concentration of cobalt salt in the solution can compensate for its low standard potential compared to the standard potential of zinc metal. In this case, it is possible to be deposited at the same time. The content of TiO_2 decreased in the electrolyte C compared to the electrolyte B.

Table 2.
Chemical composition of baths.

Elements	Composition A	Composition B	Composition C
$CoCl_2$	50 g/L	80 g/L	70 g/L
$ZnCl_2$	80 g/L	50 g/L	70 g/L
H_3BO_3	26 g/L	26 g/L	26 g/L
KCl	230 g/L	230 g/L	230 g/L
TiO_2	15 g/L	15 g/L	15 g/L
SDS (Sodium Dodecyl Sulphate)	2 g/L	2 g/L	2 g/L

Line scan analysis was conducted across the cross-section of the coating coated in electrolyte B (Fig. 3). The peaks show that the nanocomposite coating has precipitated from the substrate surface to the surface of the coating. Co is deposited almost uniformly from the sample surface to the coating surface, but its intensity is reduced in the middle of the coating and has less uniformity compared to Zn. TiO_2 is almost uniform from the sample surface to the coating surface; however, its uniformity is less than Zn and Co.

Fig. 4 shows the plane scan analysis of the coating representing the presence of Co, Zn, and Ti across the coating. The distribution of Co, TiO_2 and Zn across the coating is well shown in Fig. 4b-c. Deposition of TiO_2 particles between Zn-Co coating is observed in a completely dispersed manner and with lower density compared to the matrix components across the coating.

3.2. Morphology of the coatings

SEM morphology of the coatings deposited in electrolytes B and C are shown in Fig. 5. In both cases, TiO_2 is clustered between the grains of Zn-Co, and no differences are observed in the way TiO_2 particles are dispersed in the two coatings that possess different Co and Zn chloride concentrations. Clustering of TiO_2 particles in the coating increases with increasing the amount of TiO_2 in the bath has also been reported in previous research, but if the amount of TiO_2 is less than 15 g/L and about 5 g/L, a more uniform distribution is achieved. However, according to the main goal of the project, which is to form the maximum titanium dioxide in the coating, a higher concentration of this oxide in the electrolyte was used [33].

The average particle size of TiO_2 particles was also measured from the SEM micrograph. The average particle size of TiO_2 particles is equal

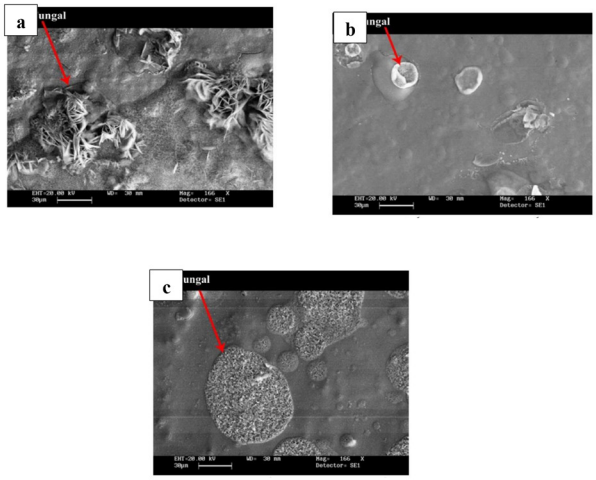

Fig. 5. SEM images of the coatings deposited in (a) electrolyte B and (b) electrolyte C.

to 20 nm. The SEM morphology showed the presence of nanoscale particles that were aggregated into fine TiO_2 spherical particles.

3.3. The adhesion of Zn-Co-TiO_2 composite coatings

Adhesion tests were performed on the Zn-Co-TiO_2 composite coatings deposited on the surface of plain carbon steel in the electrolytes A, B, and C. According to the results, the adhesions of the coatings related to electrolytes A, B, and C were 1.7 MPa, 2.23 MPa, and 1.4, respectively. As known, zinc in the electrical coating in a chloride bath is deposited as a soft coating on the steel surface, which has low adhesion and is removed in the form of laminates from the surface by applying force. Increasing Co metal in the coating causes an increase in the adhesion of the Zn coating, which has been mentioned in previous research [33, 34]. The addition of Co to the coating increases the corrosion resistance as well as its strength, but the incorporation of TiO_2 particles in the coating, which has no bond with Zn and Co, makes the coating brittle. Therefore, a higher percentage of TiO_2 causes breaking and reduction of adhesion due to the application pull-off test. Increasing Co in the coating increases the adhesion of the Zn coating, which has been observed in research conducted previously [34].

3.4. Antifungal properties of Zn-Co-TiO_2 composite coatings

To investigate the photocatalytic properties of TiO_2, fungal growth on the surface of the sample was used. First, the photocatalytic properties of TiO_2-Co-Zn nanocomposite coating under the conditions of coating formation in electrolyte A were determined. Since the amount of TiO_2 in this coating is very low, it has a negligible effect on preventing the growth of fungi on the surface of the samples. Fig. 6 also shows that fungus eggs in the container are growing on the sample surface. Titanium nanoparticles that became semiconductors by ultraviolet photons generate charge and produce free radicals, causing fungi to compose remove. Furthermore, titanium dioxide forms non-toxic decomposition products that pose no risk to the environment.

In electrolyte B, at the current intensity of 0.1, A due to the maximum amount of TiO_2 compared to other electrolytes, reduced growth of fungal eggs was observed. Since the maximum amount of TiO_2 in the coating is higher, more free radicals are formed upon ultraviolet light radiation. According to Fig 6 a, in electrolyte C, fungal eggs growth increases due to the minimum amount of TiO_2 [35].

Table 3.
Elemental analysis of the coatings deposited in various electrolytes.

Element	Electrolyte A (wt%)	Electrolyte B (wt%)	Electrolyte C (wt%)
TiO_2	0.91	4.16	1.62
Co	0.49	10.24	6.67
Zn	98.60	85.60	91.69

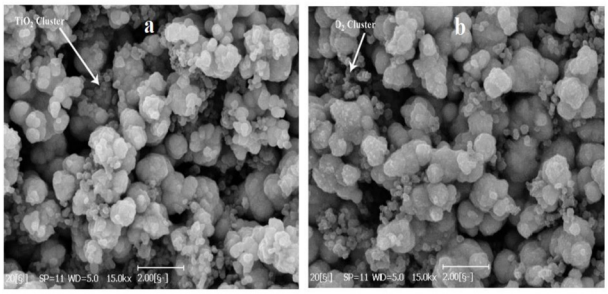

Fig. 6. SEM image of fungal growth in (a) electrolyte A, (b) electrolyte B, (c) electrolyte C.

4. Conclusions

In this paper, electrodeposited nanocomposite coatings of Zn-Co-TiO_2 were applied on a steel substrate with the advantage of being cost-effective. The Zn, Co and, TiO_2 are biocompatible metals that were used to prepare Zn-Co-TiO_2 nanocomposite coating. The effect of the addition of TiO_2 nanoparticles and different electrolyte compositions on the morphology, adhesion strength, and photocatalytic activity of the coating was evaluated. The results showed that electrolyte B with Zn and CO chloride salts in concentrations of 50 and 80 g/l, respectively, rendered the highest amounts of Zn and Co metals along with TiO_2 in the coating. The addition of Co to the coating increases the corrosion resistance as well as its strength, but the incorporation of TiO_2 particles in the coating, which has no bond with Zn and Co, makes the coating brittle. By increasing the amount of TiO_2, the photocatalytic properties and decomposition of fungi also increased.

REFERENCES

[1] E. Rosolymou, S. Spanou, C. Zanella, D.S. Tsoukleris, S. Köhler, P. Leisner, E.A. Pavlatou, Electrodeposition of Photocatalytic Sn–Ni Matrix Composite Coatings Embedded with Doped TiO_2 Particles, Coatings 10(8) (2020) 775.
[2] H. Li, P. Wang, X. Yi, H. Yu, Edge-selectively amidated graphene for boosting H2-evolution activity of TiO_2 photocatalyst, Applied Catalysis B: Environmental 264 (2020) 118504.
[3] M.S.F.A. Zamri, N. Sapawe, Regeneration studies of TiO_2 photocatalyst for degradation of phenol in a batch system, Materials Today: Proceedings 19 (2019) 1327-1332.
[4] A. Daniyan, L. Umoru, O. Fayomi, A. Popoola, Structural evolution, optoelectrical and corrosion properties of electrodeposited WO_3 integration on Zn-TiO_2 electrolyte for defence super application, Defence Technology 14(5) (2018) 396-402.
[5] F. Qi, H. Li, Z. Yang, J. Zhao, Y. Hu, H. Liu, Efficient reduction of CO_2 to CO by Ag3PO4/TiO_2 photocatalyst under ultraviolet and visible light irradiation, Asia-Pacific Journal of Chemical Engineering 15(5) (2020) e2499.
[6] Y.W. Song, S.E. Kim, Y.G. Jung, J.Y. Yoo, J.C. Park, Controlling Nitrogen Oxide and Ultraviolet-A irradiance in ventilation duct system using TiO_2 photocatalyst, Building and Environment 199 (2021) 107881.
[7] M. Miyauchi, K. Sunada, K. Hashimoto, Antiviral effect of visible light-sensitive Cu_xO/TiO_2 photocatalyst, Catalysts 10(9) (2020) 1093.
[8] Z. Lodhi, J. Mol, W. Hamer, H. Terryn, J. De Wit, Cathodic inhibition and anomalous electrodeposition of Zn–Co alloys, Electrochimica acta 52(17) (2007) 5444-5452.
[9] G. Roventi, T. Bellezze, R. Fratesi, Electrochemical study on the inhibitory effect of the underpotential deposition of zinc on Zn–Co alloy electrodeposition, Electrochimica Acta 51(13) (2006) 2691-2697.
[10] R.S. Bhat, V.B. Shet, Development and characterization of Zn–Ni, Zn–Co and Zn–Ni–Co coatings, Surface Engineering 36(4) (2020) 429-437.
[11] M. Riđošić, E. García-Lecina, A. Salicio-Paz, J. Bajat, The advantage of ultrasound during electrodeposition on morphology and corrosion stability of Zn-Co

alloy coatings, Transactions of the IMF 98(3) (2020) 114-120.
[12] P. Bajaj, A. Hariharan, A. Kini, P. Kürnsteiner, D. Raabe, E.A. Jägle, Steels in additive manufacturing: A review of their microstructure and properties, Materials Science and Engineering: A 772 (2020) 138633.
[13] I. Sknar, Y. Sknar, T. Hrydnieva, P. Riabik, O. Demchyshyna, D. Gerasimenko, Development of a New Suspension Electrolyte Based on Methanesulphonic Acid for the Electrodeposition of Cu–TiO_2 Composites, Eastern-European Journal of Enterprise Technologies 1(6) (2021) 109.
[14] R. Wadhene, A. Lamouchi, I.B. Assaker, J.B. Naceur, M. Martínez-Huerta, R. Chtourou, Electrodeposition of Cu2ZnSnS4 thin films onto TiO_2 nanorods for photocatalytic application: Effect of deposition time, Inorganic Chemistry Communications 122 (2020) 108298.
[15] R. Fratesi, G. Roventi, G. Giuliani, C. Tomachuk, Zinc–cobalt alloy electrodeposition from chloride baths, Journal of Applied Electrochemistry 27(9) (1997) 1088-1094.
[16] H. Wei, Y.-l. Chen, W. Yu, L. Su, X. Wang, D. Tang, Study on corrosion resistance of high-strength medium-carbon spring steel and its hydrogen-induced delayed fracture, Construction and Building Materials 239 (2020) 117815.
[17] M. Jung, G. Lee, J. Choi, Electrochemical plating of Cu-Sn alloy in non-cyanide solution to substitute for Ni undercoating layer, Electrochimica Acta 241 (2017) 229-236.
[18] B. Li, W. Zhang, D. Li, Y. Huan, J. Dong, Microstructural, surface and electrochemical properties of a novel Ni–B/Ni–W–BN duplex composite coating by co-electrodeposition, Applied Surface Science 458 (2018) 305-318.
[19] I. Bobowska, A. Wypych-Puszkarz, A. Opasinska, W. Maniukiewicz, P. Wojciechowski, Effect of heat treatment on the structure and morphology of ZnO nanorod array and its composite with titania precursor, Phase Transitions 90(1) (2017) 44-53.
[20] O. Fayomi, A. Popoola, Anti-corrosion properties and structural characteristics of fabricated ternary coatings, Surface Engineering and Applied Electrochemistry 51 (2015) 76-84.
[21] M. Diafi, A. Aidi, B. Benhaoua, Study of Zn–Co alloy coatings modified by nano-TiO_2 particles incorporation, Digest Journal of Nanomaterials & Biostructures (DJNB) 15(3) (2020).
[22] G. Mohammadnezhad, M.M. Momeni, F. Nasiriani, Enhanced photoelectrochemical performance of tin oxide decorated tungsten oxide doped TiO_2 nanotube by electrodeposition for water splitting, Journal of Electroanalytical Chemistry 876 (2020) 114505.
[23] M. Shourgeshty, M. Aliofkhazraei, A. Karimzadeh, R. Poursalehi, Corrosion and wear properties of Zn–Ni and Zn–Ni–Al_2O_3 multilayer electrodeposited coatings, Materials Research Express 4(9) (2017) 096406.
[24] M. Ibrahim, J.B. Agboola, A.S. Abdulkareem, O. Adedipe, J.O. Tijani, Anti-Corrosion Behaviour of Silver-Cobalt Oxide-Titanium Dioxide Nanocomposites Coated Mild Steel in Sea water, Federal University Oye (FUOYE) Journal of Engineering and Technology (FUOYEJET), 5(2) (2020) 159-164.
[25] M. Amiriafshar, M. Rafieazad, X. Duan, A. Nasiri, Fabrication and coating adhesion study of superhydrophobic stainless steel surfaces: The effect of substrate surface roughness, Surfaces and Interfaces 20 (2020) 100526.
[26] I.-D. Utu, R. Muntean, I. Mitelea, Corrosion and Wear Properties of Zn-Based Composite Coatings, Journal of Materials Engineering and Performance 29(8) (2020) 5360-5365.
[27] J.E.A. Qudeiri, A. Zaiout, A.-H.I. Mourad, M.H. Abidi, A. Elkaseer, Principles and characteristics of different EDM processes in machining tool and die steels, Applied Sciences 10(6) (2020) 2082.
[28] D.S. Kharitonov, A.A. Kasach, D.S. Sergievich, A. Wrzesińska, I. Bobowska, K. Darowicki, A. Zielinski, J. Ryl, I.I. Kurilo, Ultrasonic-assisted electrodeposition of Cu-Sn-TiO_2 nanocomposite coatings with enhanced antibacterial activity, Ultrasonics Sonochemistry 75 (2021) 105593.
[29] S. Nasibi, K. Alimohammadi, L. Bazli, S. Eskandarinezhad, A. Mohammadi, N. Sheysi, TZNT alloy for surgical implant applications: A systematic review, Journal of Composites and Compounds 2(3) (2020) 62-68.
[30] A. Najafidoust, S. Allahyari, N. Rahemi, M. Tasbihi, Uniform coating of TiO_2 nanoparticles using biotemplates for photocatalytic wastewater treatment, Ceramics International 46(4) (2020) 4707-4719.
[31] F. Da Silva, N. Cinca, S. Dosta, I. Cano, J.M. Guilemany, C. Caires, A. Lima, C. Silva, S. Oliveira, A. Caires, Corrosion resistance and antibacterial properties of copper coating deposited by cold gas spray, Surface and Coatings Technology 361 (2019) 292-301.
[32] W. Zhang, T. Mei, B. Li, L. Yang, S. Du, Y. Miao, H. Chu, Effect of current density and agitation modes on the structural and corrosion behavior of Ni/diamond composite coatings, Journal of Materials Research and Technology 12 (2021) 1473-1485.
[33] A. Pop, A. Vlasa, S. Varvara, B. David, C. Bulea, L. Muresan, Structural and electrochemical characterization of Zn-TiO_2 nanocomposite coatings electrodeposited on steel, Optoelectronics and Advanced Materials, Rapid Communications 3 (2009) 1290-1294.
[34] C. Panagopoulos, D. Lagaris, P. Vatista, Adhesion and corrosion behaviour of Zn–Co electrodeposits on mild steel, Materials Chemistry and Physics 126(1-2) (2011) 398-403.
[35] Z. Zhang, J. Tang, Y. Wang, H. Wang, B. Normand, Y. Zuo, Electrodeposition of a Pd-Ni/TiO_2 composite coating on 316L SS and its corrosion behavior in hot sulfuric acid solution, Coatings 8(5) (2018) 182.